1

Mixing and Its Role in the Ocean

1.1 Overview

Defined in dictionaries as the 'combining of things so the resulting substance is uniform in composition, whether or not the separate elements can be distinguished', 'mixing' is often a general term that depends on the length scales being considered. In the North Atlantic, 100 km-diameter eddies are viewed as mixing agents when they reduce variability across the Gulf Stream. Mixing, however, is not complete until molecular viscosity smoothes velocity fluctuations to remove significant shear. Consequently, the viscous dissipation rate,

$$\epsilon \equiv \nu\overline{(\nabla \mathbf{v}')^2} \quad \left[\mathrm{W\,kg^{-1}}\right], \tag{1.1}$$

is the fundamental parameter of turbulence, as it equals the flux of energy from large to small scales when turbulence is at steady state. In stratified fluids, fluctuations of temperature and salinity produced by turbulence are smoothed at rates parameterized by

$$\chi_\mathrm{T} \equiv 2\kappa_T\overline{(\nabla \Theta')^2} \quad \left[\mathrm{K^2\ s^{-1}}\right], \tag{1.2}$$

$$\chi_\mathrm{S} \equiv 2\kappa_S\overline{(\nabla S')^2} \quad \left[\mathrm{s^{-1}}\right], \tag{1.3}$$

where Θ is conservative temperature (Section 2.2.2), S is salinity in parts per thousand,[1] and primes denote fluctuations about means. In the ocean, these variances are contributed by gradients over tens of centimeters to fractions of a millimeter. How this happens in the stratified ocean is the focus of this book.

Storage and transport of heat in the ocean, the flywheel of global climate, is a major concern of climatologists, who in turn rely on oceanographers to

[1] In this form, χ_S is proportional to $(\mathrm{g_{ss}/kg_{sw}})^2\ \mathrm{s^{-1}}$ where $\mathrm{g_{ss}}$ is grams of sea salt and $\mathrm{kg_{sw}}$ is kilograms of seawater. If the salinity gradient were in concentration units, represented by s, the proportionality would be to $(\mathrm{kg_{ss}/kg_{sw}})^2\ \mathrm{s^{-1}}$.

estimate bulk mixing coefficients from measurements of centimeter-scale gradients contributing to ϵ, χ_T, and χ_S. The scales at which this occurs are determined by the intensity of the turbulence, ϵ, and the properties of seawater (Chapter 2). Termed 'microstructure', these length scales are the smallest of physical significance in the ocean. How the measurements are made (Chapter 5), the assumptions and uncertainties accompanying them (Chapter 3), and their relation to larger-scale processes producing microstructure are the core of mixing research.

Two processes, double diffusion (Chapter 4) and internal waves, produce nearly all microstructure mixing the pycnocline. Double diffusion is driven by the 100-fold contrast in molecular diffusivities of heat and salt. In addition to forming convecting layers when stable cool fresh water overlies warm saline water, double diffusion generates centimeter-diameter salt fingers when the vertical gradients are reversed. A few centimeters in diameter under oceanic conditions, salt fingers can form staircases when their fluxes are intense. One of the major issues, however, is the contribution of salt fingers to heat and salt fluxes over large areas of the pycnocline where fingering does not form staircases. In these situations fingers are difficult to detect in profiles but have been observed in horizontal measurements.

Internal waves, the second process, are mostly generated at the sea surface by wind and at the seafloor by low-frequency currents over rough bottoms (Chapter 6). As they propagate from the boundaries, internal waves transport energy vertically as well as horizontally, creating patches of turbulence as they break. Viscosity dissipates the turbulence and enhances heat and salt diffusion by straining their mean gradients until diffusion smoothes them.

Numerical models of ocean circulation or even regional models have little use for the dissipation rates that are the most direct results of microstructure measurements. Rather, assuming that vertical turbulent fluxes depend linearly on background gradients, small-scale mixing is represented in models by turbulent, a.k.a. eddy, diffusivities times the mean gradients, e.g. the vertical turbulent heat flux is

$$J_Q^z = -\rho c_p K_T \partial \overline{T}/\partial z \quad \left[\mathrm{W\,m^{-2}}\right], \tag{1.4}$$

where ρ is the density of seawater, c_p is the specific heat of seawater at constant pressure, and K_T is the eddy coefficient, or turbulent diffusivity, for heat. Unlike molecular diffusivities, which depend only on the temperature, salinity, and pressure of the water, eddy diffusivities also depend on the intensity and structure of the turbulence. Presently, eddy diffusivities are estimated from microstructure by assuming that the average rate of turbulent production balances the average rate of its dissipation by viscosity or by scalar diffusion. For example,

$$K_T \approx \chi_T/2(\partial\overline{\theta}/\partial z)^2 \quad \left[\mathrm{m^2\,s^{-1}}\right], \tag{1.5}$$

is the eddy diffusivity for heat in terms of one microstructure parameter, χ_T, and the mean gradient of potential temperature (Section 3.11.2). The equivalent production–dissipation balance for turbulent kinetic energy leads to

$$K_\rho = \Gamma_{\text{mix}}\, \epsilon / N^2 \quad \left[\text{m}^2\ \text{s}^{-1}\right] \tag{1.6}$$

for the diapycnal eddy coefficient for density, K_ρ, with Γ_{mix} as the mixing coefficient, a measure of the efficiency of stratified turbulence. Owing to the ad hoc nature of this procedure, it has been tested multiple times by comparison with diffusivities inferred from the vertical thickening of artificial tracers injected into the pycnocline (Sections 3.12.1 and 5.8). Verification within a factor of two by these tests is the principal justification for accepting diffusivities from microstructure.

Although microstructure measurements are the basis for quantifying mixing, they are too limited to cover the expanse of the ocean. Fortunately, mixing produced by internal waves can be usefully estimated from finescale, loosely defined as 1–100 m, measurements of shear and strain using models of the rate at which wave–wave interactions transfer energy to small scales and ultimate dissipation (Chapter 7). Applying these models to large archives of data collected for other purposes has provided the first global maps of mixing intensity (Chapter 8). In addition to revealing variability with latitude, depth, season, and bottom roughness in the pycnocline of the open ocean, these maps reveal the uniqueness of regimes like the Southern Ocean and the Arctic.

Other than demonstrating that mixing in the pycnocline occurs episodically in patches, measurements to date provide limited insight into specifics of how the mixing evolves as internal waves break. Therefore, present understanding is also based on inferences from large-scale ocean variability, analytic and numerical models, finescale measurements, and process studies. Although much has been learned from these varied approaches, described in Section 1.2, one of the major mixing issues, the meridional overturning circulation, is not well understood. It is examined in Section 1.3, beginning with the formation of Antarctic Bottom Water (AABW) and continuing through a sequence of approaches taken to quantify its upwelling. Finally, the global levels of mixing required to uplift bottom water are constrained by the rates at which energy and scalar variability are produced in the ocean (Section 1.4).

1.2 How is Mixing Studied?

Mixing is studied by inferences, microstructure and tracer observations, proccess studies, finestructure observations, and integrated programs. Before the 1960s, microstructure could not be detected, and mixing was inferred from observations over larger scales. Although detailed measurements now anchor our understanding,

they are not sufficient by themselves. Rather, what we know is a composite formed from these related endeavors, which in the end must converge to the same understanding of how the ocean is mixed.

1.2.1 Inferences

Where oceanic regimes are dominated by one-dimensional dynamics, simplified momentum or heat equations can be used to infer turbulent, a.k.a. eddy, coefficients. Ekman (1905) pioneered this approach when he realized that the near-surface spiral he calculated was much too compressed using molecular viscosity. He resolved the discrepancy by replacing molecular viscosity with an eddy coefficient large enough to obtain a reasonable length scale. Of equally enduring significance, Munk (1966) simplified the heat equation of the abyssal Pacific thermocline to a vertical balance between turbulent diffusion and steady upwelling of AABW (Figure 1.1, left). For the assumed rate of upwelling, fitting the exponential solution to the observed profile yielded a constant eddy diffusivity of $K_T \sim 10^{-4}$ m^2 s^{-1}, a value subsequently known as the 'canonical eddy diffusivity'. In the stratified ocean, K_T and the related scalar eddy diffusivities K_S and K_ρ operate on the background stratification and are thus are of primary importance to the general circulation.

Other inferences considered bottom water flowing through deep basins, where the principal interaction was mixing with overlying warmer water (Figure 1.1, middle). As an example, inferences from temperature changes through Romanche Fracture Zone gave $K_T \sim 10^{-1}$ m^2 s^{-1}, three orders of magnitude more intense than the canonical value (Ferron et al., 2003), but consistent with direct microstructure measurements. Finally, warming of the seasonal thermocline by vertical turbulent diffusion (Figure 1.1, right) has been modeled by equating the diffusive term with the time derivative of temperature. As computational capabilities have improved, elaborate inverse methods have largely replaced simple inferences (Wunsch,

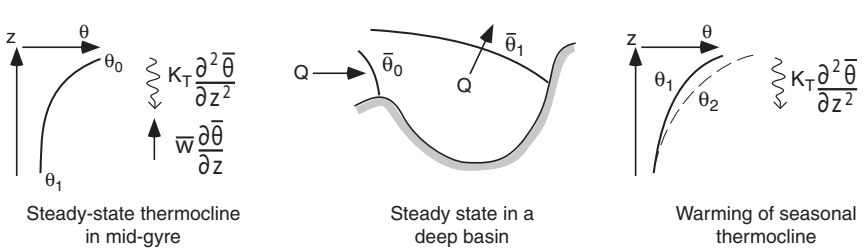

Figure 1.1 Inferences of thermal eddy coefficients for (left) a steady-state main thermocline with constant upwelling, (middle) changes in water flowing through a basin, and (right) warming of a seasonal thermocline.

2006), but the goal remains the same, to develop physical models consistent with observations.

1.2.2 Microstructure and Tracer Observations

The first successful turbulence measurements in seawater were made by towing hot-film velocity probes in a turbulent tidal channel (Grant et al., 1959). Profiling, however, soon dominated microstructure observations in the open ocean, first with untethered free-fall tubes and later with loosely tethered packages. The profiles revealed a wide range of mixing levels, with the most intense turbulence occurring in estuaries. Typical results showed ϵ and χ_T in relation to velocity and density (Figure 1.2). Now, microstructure probes are widely deployed on floats, gliders, autonomous vehicles, and moorings. Sensors have not evolved at a similar rate, but when deployed in clusters, measurements from multiple platforms are providing detailed information about mixing in mesoscale structures and in long time series.

In contrast to instantaneous mixing rates from microstructure, the spread of artificial tracers yields net mixing between observations. Artificial tracers have been injected into pycnoclines several times to test procedures for estimating eddy

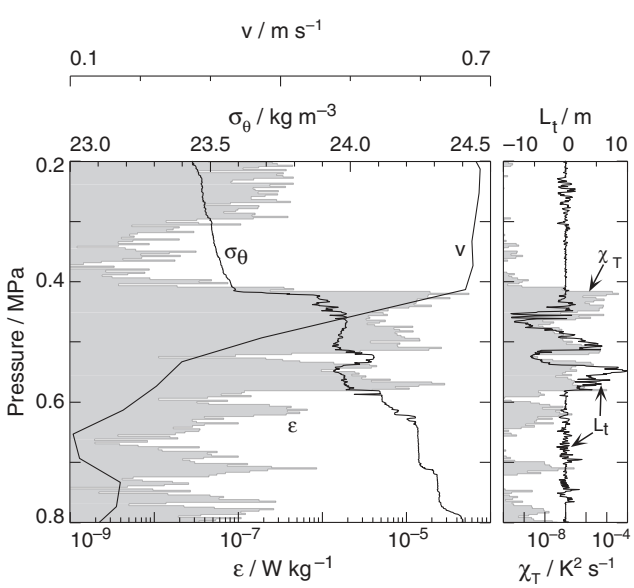

Figure 1.2 (Left) Along-channel velocity, v, potential density, σ_θ, and viscous dissipation rate, ϵ, through an overturn in profile 5854 in Figure 1.4 from Admiralty Inlet. (Right) Overturning displacements, L_t, and the rate of thermal dissipation, χ_T. Pressures 0.2–0.8 MPa correspond to depths of 20–80 m. (Data from Seim and Gregg, 1994)

diffusivities from microstructure (Section 5.8). Releases in coastal waters were observed for weeks, and those in the open ocean for months. In all cases, net diffusivities agreed within a factor of two with microstructure estimates. These comparisons are the principal justification for believing the ad hoc procedures for inferring diffusivity from dissipation rates.

1.2.3 Process Studies

Owing to the ease with which double diffusivity staircases were disrupted in laboratory tanks (Stern, 1960) and the belief that the pycnocline is moderately or strongly turbulent, double diffusion was initially treated as a curiosity rather than as an important oceanic process. Nonetheless, extensive laboratory studies (Turner, 1973) explored it and quantified buoyancy fluxes across staircase interfaces (Chapter 4). Subsequent observations, however, indicate that oceanic staircases formed by salt fingering differ in important respects from those in laboratories. Some analytic models address these issues, but a major need now is more detailed observations of staircases at sea. The more important unknown, though, is the role of fingering where it is does not form staircases. Some microstructure-based estimates suggest that fingers may contribute half the vertical flux in typical pycnoclines lacking staircases, and patches of fingers have been observed. Owing to the scale of the internal waves affecting the fingers, they cannot be simulated accurately in laboratories. Thus, laboratory experiments with double diffusion appear to have run their course, and the hope is for realistic simulations including fingers and the large-scale internal waves affecting them.

Visual identification of shallow internal waves breaking as Kelvin–Helmholtz shear instabilities (Woods, 1968) spawned a continuing sequence of laboratory and numerical studies seeking to understand mixing during these episodic events. For instance, Figure 1.3 illustrates where density instabilities develop in overturning billows. A major goal of laboratory and numerical studies of shear instabilities is to determine Γ_{mix} and its dependence on the strength and age of the instability. Other than by comparing microstructure and tracer spreading rates, mixing efficiency has not been determined in the ocean, as it requires simultaneous observations of microstructure and changes in potential energy. Numerical simulations can in principle do this, but those to date have concentrated on thin interfaces separating homogenous layers. The pycnocline, however, is irregularly steppy, with high gradients bounded by lesser gradients that nonetheless are well stratified and provide paths for small internal waves generated by the instabilities to propagate away, removing some of the energy.

The most successful mixing process studies to date modeled, analytically and numerically, the rate of energy transfer by interactions between internal waves

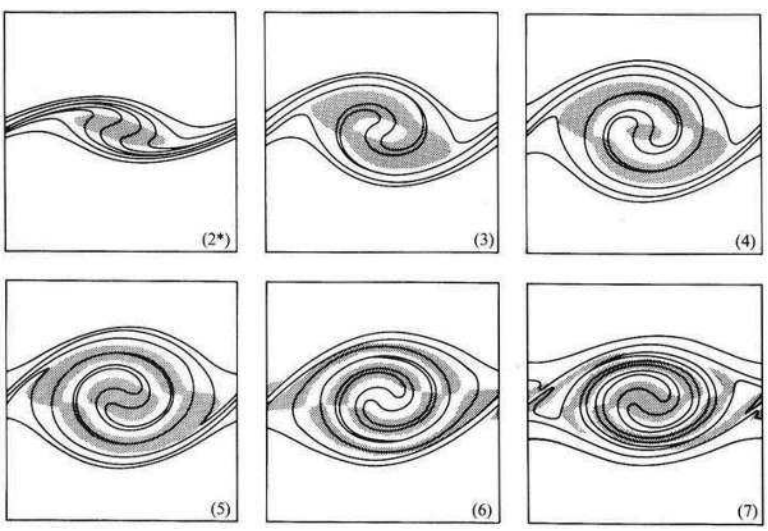

Figure 1.3 Simulation of a Kelvin–Helmholtz instability, shown initially when instabilities develop (2*), marked by shading. The Reynolds number was 500 at times of maximum (3) and minimum (6) Reynolds number stress, maximum kinetic energy (4), and zero Reynolds stress (5 & 7). (From Klaassen and Peltier, 1985).

(Section 7.5). These calculations demonstrated a net energy flux from large to small scales, which at steady state equals the turbulent dissipation rate, ϵ, produced by breaking internal waves. Formulation of the flux in terms of background stratification and internal wave shear and strain enables estimation of dissipation rates from finescale measurements.

1.2.4 Finestructure Observations

Finescale measurements relate mixing patches to the structures creating them, including the mean gradients needed for estimating eddy coefficients. They, however, do not usually resolve lateral variability well enough to identify mixing structures. Where strong stratification exists in estuaries and near coasts, unaliased images of strong events can be obtained using tow chains or backscatter from narrow beams of high-frequency acoustics. The example in Figure 1.4 shows a train of overturning billows similar to Kelvin–Helmholtz instabilities in laboratories, with the the profile in Figure 1.2 passing through an overturn. The image was essential in identifying the nature of the mixing patch.

In addition to being background for microstructure, finestructure contains the information needed to apply parameterizations from process studies to estimate mixing rates in most of the ocean. This allows mixing to be estimated within a factor of two from finescale profiles collected during large-scale surveys, as well as

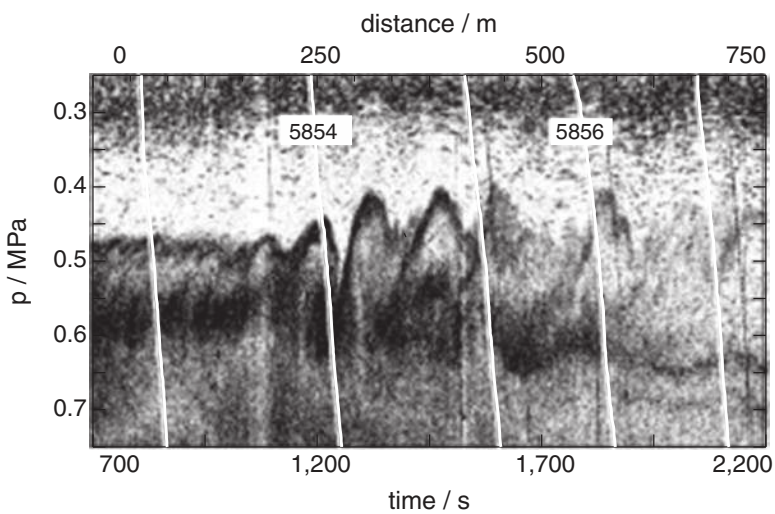

Figure 1.4 Intensity of 200 kHz acoustic backscatter from overturning billows in Admiralty Inlet. The track of profile 5854 from Figure 1.2 is labeled. By homogenizing the water, the intense mixing reduced backscatter amplitude by profile 5857. (Adapted from Seim and Gregg, 1994)

from the 4,000 Argo floats taking temperature and salinity profiles throughout the ocean every ten days. The results led to the first global estimates of mixing rates (Section 8.4).

1.2.5 Integrated Studies

Early mixing studies were often solo affairs, sampling microstructure and a few finescale variables from one ship during a few weeks in a small area. As measurements became more reliable and more accepted, microstructure was included in large-scale experiments, e.g. Polymode, but it was incidental to program goals. More recent programs include microstructure as an essential component. One example, the Hawaii Ocean Mixing Experiment (HOME) (Section 8.9.2), was inspired by satellite observations of coherent internal tides radiating from the islands. Subsequent modeling predicted the sources, and intensive observations verified the predictions, in addition to estimating accompanying local mixing. A successor program followed one of the northward internal tide beams to examine its effect on mixing far from the islands.

Owing to the importance of the Southern Ocean to heat and carbon transfer between atmosphere and ocean, several programs have addressed locations expected to mix intensely (Section 8.7). The Diapycnal and Isopycnal Mixing Experiment (DIMES) focused on Drake Passage, while the Southern Ocean

Finestructure Experiment (SOFine) worked around Kerguelen Plateau, two of the three sites providing the principal drag on the Antarctic Circumpolar Current (ACC), which flows unimpeded around the globe, driven by strong zonal winds. Seeking a comprehensive understanding, these programs included modeling, moorings, sections of fine and microstructure profiles, analysis of satellite data, and a tracer release. Observations and insights discussed in subsequent chapters have come from all of these types of programs.

1.3 The Meridional Overturning Circulation

Circling the globe between 1872 and 1876 on the first modern oceanographic expedition, *H.M.S. Challenger* traced the densest bottom water to Antarctica (Figure 1.5). Decreasing density of AABW as it flows north is evidence of mixing, but how and where it upwells remains a major issue. Present understanding of the overturning circulation includes northward bottom flows, upwelling in the three ocean basins, and shallow return flows. Mixing is central to forming the dense water, modifying it during descent, and subsequently lifting it to depths reached by wind-driven upwelling.

1.3.1 Formation of Antarctic Bottom Water (AABW)

Bottom water is formed at a few sites around Antarctica where polynyas, persistent ice-free bands, expose seawater on the continental shelf to winter winds off the continent (Figure 1.6). Owing to the difficulty in observing these locations,

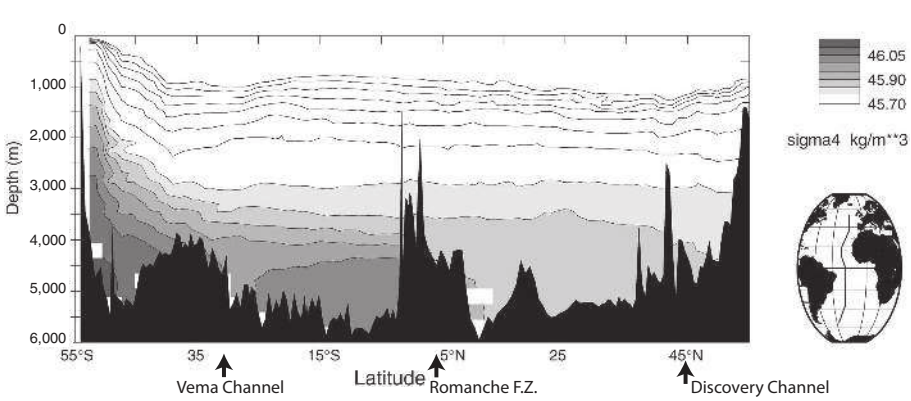

Figure 1.5 Potential density along a meridional section in the Atlantic. As AABW flows north, its density decreases abruptly in narrow gaps between basins. (From Bryden and Nurser, 2003. © American Meteorological Society. Used with permission)

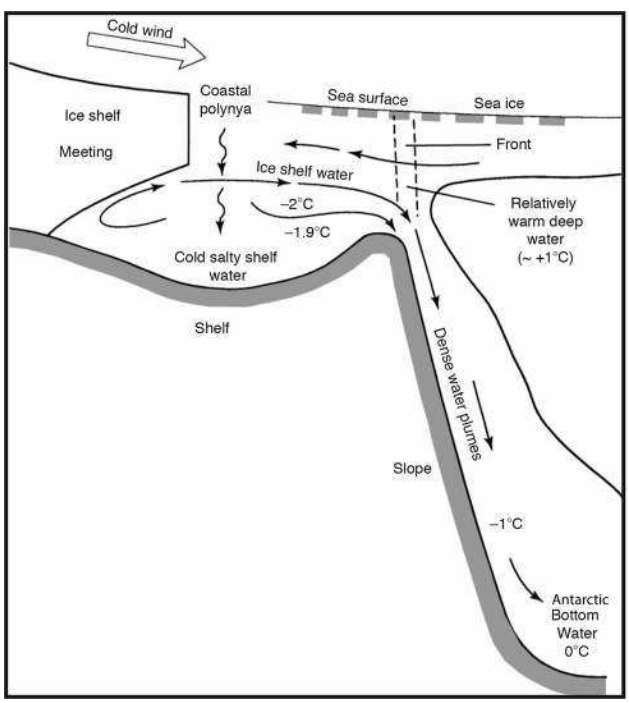

Figure 1.6 Schematic formation of AABW by convection in polynyas and further cooling under ice sheets before cascading down the slope. (Adapted from Gordon, 2013)

measurements have been limited to hydrography, which indicates that, after sinking during surface convection, shelf water is further cooled by the undersides of floating ice sheets. With temperatures as low as –2°C, the dense water flows over the shelf edge and sinks, reaching great depths when salinity exceeds 34.61.

Sinking is enhanced by cabbeling and thermobaricity (Foster, 1972; Klocker and McDougall, 2010), which result from nonlinearities in density as a function of temperature, salinity, and pressure (Sections 2.6 and 2.9). Descending the continental slope, the sinking water forms density currents entraining warmer ambient water from offshore. Entrainment approximately doubles transport to $\approx 29 \times 10^6$ m^3 s^{-1} (Talley, 2013) and can warm it to 0°C.

1.3.2 Formation of North Atlantic Deep Water (NADW)

The Indian and Pacific oceans have shallow overturning cells, with water formed in the north ultimately sinking to about 1 km, but only the North Atlantic produces water that sinks into the abyss. More accessible for observations than the Antarctic shelf, the Nordic Seas include two basins, Greenland and Norwegian,